

High-performance photorefractive polymer operating at 975 nm

Muhsin Eralp, Jayan Thomas,^{a)} Savaş Tay, Guoqiang Li, Gerald Meredith, Axel Schülzgen, and N. Peyghambarian

Optical Sciences Center, The University of Arizona, Tucson, Arizona 85721

Gregory A. Walker, Stephen Barlow,^{b)} and Seth R. Marder^{b)}

Optical Sciences Center and Department of Chemistry, The University of Arizona, Tucson, Arizona 85721

(Received 7 April 2004; accepted 9 June 2004)

A family of photorefractive polymer composites has been developed that enable high-performance device operation at a wavelength of 975 nm. This constitutes a major extension into the near-infrared spectral region for the operation of all-organic photorefractive devices. Utilizing our photorefractive materials, we demonstrate large net two-beam coupling gain of more than 100 cm⁻¹, 60% diffraction efficiency in four-wave mixing experiments, and a fast response time of 33 ms, at an irradiance of 1 W/cm². © 2004 American Institute of Physics. [DOI: 10.1063/1.1780591]

Photorefractive (PR) materials have potential applications in areas such as dynamic holography, optical processing, reversible data storage, and phase conjugation.¹ Organic PR composites offer several advantages over their inorganic counterparts due to their ease of processability, low cost, and chemical tunability.² In recent years, several impressive PR properties have been reported in the visible and borderline near-infrared region.^{2–4} Much less consideration has been given to the near-infrared (wavelength > 830 nm) region, mainly due to the unavailability of a composite with favorable PR properties that operates within this spectral range. On the other hand, this wavelength range is of major importance, e.g., for medical imaging and optical communications, and compact solid-state lasers operating in this spectral region are readily available. In a recent report on PR composites, inorganic semiconductor nanocrystals were used to achieve sensitization at 1310 nm;⁵ however, the response times in these hybrid materials are usually slow and diffraction efficiencies are much lower compared to all-organic composites.⁶ We demonstrate a proof of photorefractivity at 975 nm in an all-organic composite with a performance comparable to and possibly better than the current organic materials at 780 and 830 nm;^{7–9} a significant step towards organic PR devices at a new near-infrared wavelength.

In this letter, we focused our attention on a composite based on a polymer (PATPD) which has a polyacrylate backbone and a well-known hole-transporting tetraphenyldiaminobiphenyl type (TPD) pendant group attached through an alkoxy linker (Fig. 1). The hole transporter, PATPD, was doped with a well-known nonlinear optical (NLO) chromophore, 4-homopiperidino benzylidene-malonitrile (7-DCST), and a near-infrared dye, DBM (Fig. 1) for charge generation at the operating wavelength.^{10–12} Composites prepared include PATPD/7-DCST/ECZ/DBM (54/25/20/1 wt. %) (C1) and PATPD/7-DCST/ECZ/DBM (49/35/15/1 wt. %) (C2). C1 was phase stable for more than six months at room temperature, while in C2 crystallization was observed after a few weeks. Samples of both composites were prepared by laminating 105 μm thick layers between

glass slides with indium–tin–oxide electrodes.

Figure 1 shows the absorption coefficient of the sample C1, demonstrating sensitization at wavelengths near 1 μm. A large ratio of photoconductivity (σ_{ph}) to background conductivity (σ_{dark}) is very beneficial in PR materials since majority carriers can easily move from high to low intensity regions and get trapped leading to the formation of stronger internal space-charge fields. At low illumination, the ratio between σ_{ph} and σ_{dark} limits the strength of the space-charge field via the prefactor $\sigma_{ph}/(\sigma_{dark} + \sigma_{ph})$. Figure 1(inset) shows the photoconductivity of the composites measured using 975 nm radiation. We accounted for the light intensity attenuation due to the finite sample thickness and normalized the data with respect to the absorbed light intensity.¹³ This normalized photoconductivity also reflects the magnitude of photogeneration, carrier mobility, and lifetime. At an intensity level of 1 W/cm² and an applied field of 56 V/μm, the normalized photoconductivity of 1000 pS/cm (C1) is five orders of magnitude larger than the dark conductivity of 0.02 pS/cm (Table I).

Another crucial parameter in developing high-performance PR materials is the refractive index modulation,

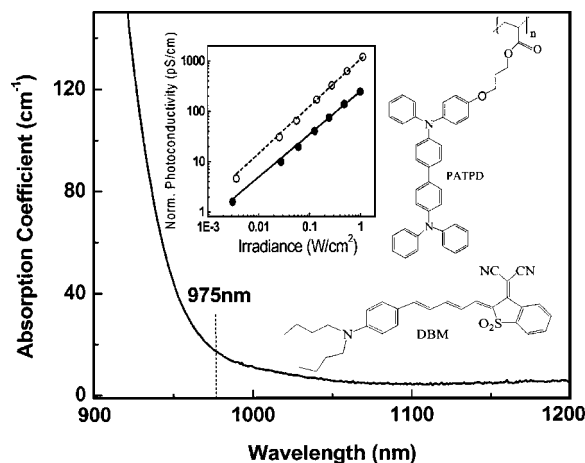


FIG. 1. Near-infrared absorption spectrum of C1 and chemical structures of polymer (PATPD) and sensitizing dye (DBM). Inset shows intensity dependence of photoconductivity for C1 (○) and C2 (●) at an electric field of 56 V/μm and at a beam intensity of 1 W/cm². The lines are a guide to the eye.

^{a)}Electronic mail: jthomas@optics.arizona.edu

^{b)}Present address: School of Chemistry and Biochemistry, Georgia Institute of Technology, Atlanta, GA 30332.

TABLE I. Photorefractive properties of composites C1 and C2. Photoconductivity σ_{photo} ; dark conductivity σ_{dark} ; birefringence Δn ; diffraction efficiency η_{max} ; fast response time τ_i ; two beam coupling gain Γ .

Composite	$\sigma_{\text{photo}}/\sigma_{\text{dark}}$ ^a (pS/cm)	Δn @ 76 V/ μm	η_{max} ^b (%)	τ_i ^c (ms)	Γ @ 76 V/ μm (cm^{-1})
C1	1000/0.02	0.0012	35	96	60
C2	240/0.06	0.0055	60	33	110

^a $E_0=56 \text{ V}/\mu\text{m}$; $I_0=1 \text{ W}/\text{cm}^2$.

^b $E_0=95 \text{ V}/\mu\text{m}$; $I_{\text{write}}(\text{total})=1 \text{ W}/\text{cm}^2$; $I_{\text{probe}}=3 \text{ mW}/\text{cm}^2$.

^c $E_0=95 \text{ V}/\mu\text{m}$; $I_{\text{write}}(\text{total})=1 \text{ W}/\text{cm}^2$; $I_{\text{probe}}=3 \text{ mW}/\text{cm}^2$.

which is primarily due to chromophore orientation (in low T_g materials). Under an applied electric field, the orientation of the NLO chromophores results in birefringence that has been measured by an ellipsometric technique.¹⁴ The relatively low index modulation in C1 (0.0012) compared to C2 (0.0055) is due to the reduced loading of the NLO chromophore (25%).

To characterize the PR properties written in the samples, four-wave mixing experiments were performed in a standard geometry. Two interfering s -polarized beams of equal fluences ($0.5 \text{ W}/\text{cm}^2$ each) were used to write the grating and a weak counterpropagating p -polarized beam ($3 \text{ mW}/\text{cm}^2$) was used as the probe beam. The writing beams were incident on the sample at an interbeam angle of 22.5° in air and the sample surface was tilted 60° relative to the writing beam bisector resulting in a grating period of $4.3 \mu\text{m}$. Figure 2 shows the diffraction efficiency (percentage of diffracted probe beam) as a function of the applied external field under stationary conditions. The internal diffraction efficiency for sample C1 increases to a maximum value of 35% at $95 \text{ V}/\mu\text{m}$ on a $105 \mu\text{m}$ thick device without reaching an overmodulation, i.e., a diffraction maximum followed by a successive decrease in diffraction efficiency. The low diffraction efficiency in C1 is caused by the low chromophore loading (25%) and the correspondingly small refractive index modulation (Table I) compared to C2. Furthermore, from the Kogelnik's equation¹⁵ for diffraction efficiency:

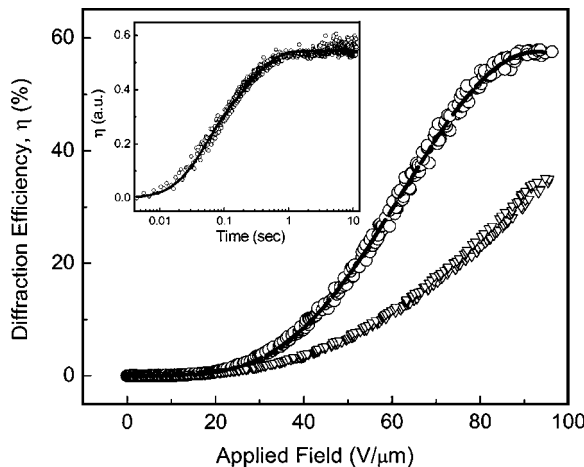


FIG. 2. Steady-state diffraction efficiency vs external electric field for C1 (▽) and C2 (○); the solid line is a theoretical fit (Ref. 14) for a trap density of $2.3 \times 10^{16} \text{ cm}^{-3}$. Transient growth of diffraction efficiency as the second beam writing turned on for C2 is shown in the inset. The solid line in the inset is a biexponential growth fit ($\tau_1=33 \text{ ms}$, $\tau_2=320 \text{ ms}$, weight factor $m=0.5$).

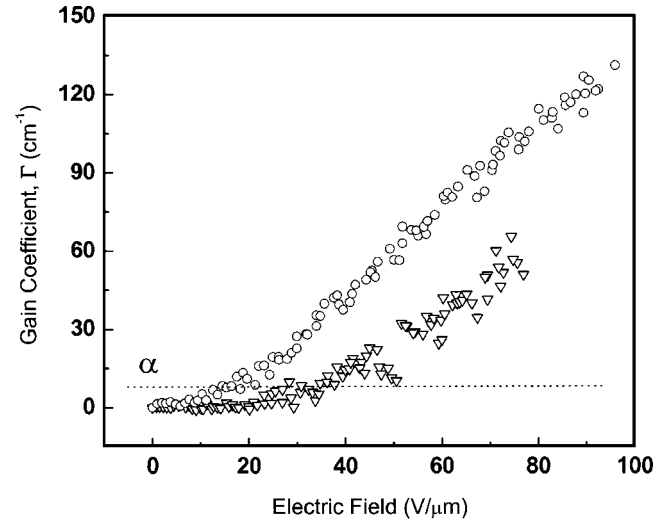


FIG. 3. Electric field dependence of two beam coupling gain coefficient of C1 (▽) and C2 (○) for p -polarized writing beams. The absorption coefficient $\alpha=13 \text{ cm}^{-1}$ is included for comparison (dotted line).

$$\eta \propto \sin^2 \left[\frac{\pi \cdot \Delta n(E) \cdot d}{\lambda (c_R \cdot c_S)^{1/2}} \right], \quad (1)$$

it is clear that at longer wavelengths, overmodulation occurs at larger index contrasts. Here, Δn is the field-dependent index modulation, d is the thickness of the film, and c_R and c_S are geometrical factors. In sample C2, however, the larger chromophore content (35%) proved sufficient to reach the overmodulation with a maximum in diffraction efficiency of 60% below $95 \text{ V}/\mu\text{m}$. On the other hand, index modulation can be limited by the trap density which affects the strength of the space-charge field. The field dependence of η can give an estimate about the effective trap density. A reasonable fit of the data to the theory¹⁶ (Fig. 2) gives a trap density of $2.3 \times 10^{16} \text{ cm}^{-3}$. From simulations based on the Kukharev model,¹⁶ we found that the present samples are in the trap limited regime and further traps are necessary to increase the index modulation of our devices.

The dynamics of the grating built-up can be extracted from a biexponential function fit that is correlated to the growth of the space-charge field.¹⁷ Figure 2 inset shows the evolution of the diffraction efficiency after switching on the second writing beam at time $t=0$ for C2. The line represents the fit to the data. Remarkably fast dynamics with characteristic time constants of 96 ms for C1 and 33 ms for C2 were observed indicating possible application of these composites in systems that operate at or close to video rates. In sample C2 these dynamics were measured at a field close to the peak of the diffraction efficiency (overmodulation point).

The unique nonlocal nature of the photorefractive grating was demonstrated by a two beam coupling experiment which is considered to be a signature of photorefractivity.¹⁸ We adapted the same tilted sample geometry with only p -polarized writing beams in a 1:1 ratio providing a total fluence of $1 \text{ W}/\text{cm}^2$. The net gain obtained for the samples are shown in Fig. 3. These measurements not only demonstrate the photorefractive nature of the light-induced gratings, but also open the door for applications where continuous redirection of energy between light beams is needed.

In summary, we have demonstrated high-performance PR polymer composites at 975 nm. PR gratings can be writ-

ten within tens of milliseconds, diffraction efficiencies from these gratings reached 60% and a two-beam coupling gain of 130 cm^{-1} were observed. The large photoconductivity suggests the possibility of achieving even faster response times within this family of polymer composites. Extending the sensitization of an all-organic photorefractive device to the wavelength of almost $1\text{ }\mu\text{m}$ represents a significant advance in the development of all-organic PR devices for near-infrared imaging and optical communication. Further research will focus on increasing the refractive-index modulation, improving the response times as well as shelf-life times of these materials, and extending the range of operating wavelengths further into the infrared region.

This research has been supported by U.S. Air Force Office of Scientific Research, National Science Foundation, Nitto Denko Technical Corporation, NSG Photonics Company and by the State of Arizona TRIF Photonics Initiative.

¹*Photorefractive Materials and Their Applications*, edited by P. Günter and J. P. Huignard (Springer, New York, 1988), Vol. 2.

²W. E. Moerner, A. Grunnet-Jepsen, and C. L. Thompson, *Annu. Rev. Mater. Sci.* **27**, 585 (1997).

³B. Kippelen, S. R. Marder, E. Hendrickx, J. L. Maldonado, G. Guillemet, B. L. Volodin, D. D. Steele, Y. Enami, Sandalphon, Y. J. Yao, J. F. Wang, H. Rockel, L. Erskine, and N. Peyghambarian, *Science* **279**, 54 (1998).

⁴D. Wright, M. A. Diaz-Garcia, J. D. Casperson, M. DeClue, W. E. Moerner, and R. J. Twieg, *Appl. Phys. Lett.* **73**, 1490 (1998).

⁵J. G. Winiazar, L. Zhang, J. Park, and P. N. Prasad, *J. Phys. Chem. B* **106**, 967 (2002).

⁶J. G. Winiazar, L. Zhang, M. Lal, C. S. Friend, and P. N. Prasad, *J. Am. Chem. Soc.* **121**, 5287 (1999).

⁷C. Engels, D. Van Steenwinckel, E. Hendrickx, M. Schaerlaekens, A. Persoons, and C. Samyn, *J. Mater. Chem.* **12**, 951 (2002).

⁸E. Mecher, F. Gallego-Gomez, H. Tillmann, H. H. Horhold, J. C. Hummelen, and K. Meerholz, *Nature (London)* **418**, 959 (2002).

⁹L. M. Wang, M. K. Ng, and L. P. Yu, *Appl. Phys. Lett.* **78**, 700 (2001).

¹⁰M. A. Díaz-García, D. Wright, J. D. Casperson, B. Smith, E. Glazer, and W. E. Moerner, *Chem. Mater.* **11**, 1784 (1999).

¹¹M. Ahlheim, M. Barzoukas, P. V. Bedworth, M. Blanchard-Desce, A. Fort, Z.-Y. Hu, S. R. Marder, J. W. Perry, C. Runser, M. Staehelin, and B. Zysset, *Science* **271**, 335 (1996).

¹²M. Blanchard-Desce, V. Alain, P. V. Bedworth, S. R. Marder, A. Fort, C. Runser, M. Barzoukas, S. Lebus, and R. Wortmann, *Chem.-Eur. J.* **3**, 1091 (1997).

¹³O. Ostroverkhova, W. E. Moerner, M. He, and R. J. Twieg, *Appl. Phys. Lett.* **82**, 3602 (2003).

¹⁴B. Kippelen, Sandalphon, K. Meerholz, and N. Peyghambarian, *Appl. Phys. Lett.* **68**, 1748 (1996).

¹⁵H. Kogelnik, *Bell Syst. Tech. J.* **44**, 2909 (1969); R. Bittner, C. Brauchle, and K. Meerholz, *Appl. Opt.* **37**, 2843 (1998).

¹⁶N. V. Kukharev, V. B. Markov, S. G. Odulov, M. S. Soskin, and V. L. Vinetskii, *Ferroelectrics* **22**, 949 (1979).

¹⁷J. A. Herlocker, K. B. Ferrio, E. Hendrickx, B. D. Guenther, S. Mery, B. Kippelen, and N. Peyghambarian, *Appl. Phys. Lett.* **74**, 2253 (1999).

¹⁸C. A. Walsh and W. E. Moerner, *J. Opt. Soc. Am. B* **9**, 642 (1992).